Joint Diseases and Related Surgery

Jt Dis Relat Surg
2026;37(x):i-xv

ORIGINAL ARTICLE

Dose-dependent protective effects of punicalagin on steroid-induced osteonecrosis in a rat model

Muhammed Uslu, MD[1], Ozancan Biçer, MD[1], Yiğit Önaloğlu, MD[2], Emincan Balcı, MD[1], Yiğit Güleryüz, MD[1], Abdurrahman Acar, MD[1], Mustafa Fatih Daşcı, MD[3], Ender Alagöz, MD[3]

[1]Department of Orthopedics and Traumatology, University of Health Sciences, Bağcılar Training and Research Hospital, İstanbul, Türkiye
[2]Department of Orthopedics and Traumatology, University of Health Sciences, Başakşehir Çam and Sakura City Hospital, İstanbul, Türkiye
[3]Department of Orthopedics and Traumatology, Medipol Mega University Hospital, İstanbul, Türkiye

Osteonecrosis (ON), also known as avascular or aseptic necrosis, is characterized by bone cell death caused by a reduction or interruption in blood flow to the bone, originating from traumatic or atraumatic sources.[1-5] The femoral head is the most frequently affected site due to its limited collateral circulation. Osteonecrosis of the femoral head (ONFH) is characterized by a compromised subchondral microcirculation, particularly in the small retinacular vessels, which ultimately leads to necrosis of bone.[6] In non-traumatic cases, alcohol consumption and corticosteroid use are among the most common etiological factors.[2-4]

Since the 1950s, corticosteroids have been widely used for their immunomodulatory and anti-inflammatory properties in the treatment of various diseases. Recent studies have also

Received: January 02, 2026
Accepted: May 04, 2026
Published online: June 12, 2026

Correspondence: Muhammed Uslu, MD. SBÜ, Bağcılar Eğitim ve Araştırma Hastanesi, Ortopedi ve Travmatoloji Kliniği, 34200 Bağcılar, İstanbul, Türkiye.

E-mail: dr.muhammeduslu@gmail.com

Doi: 10.52312/jdrs.2026.2795

Citation: Uslu M, Biçer O, Önaloğlu Y, Balcı E, Güleryüz Y, Acar A, et al. Dose-dependent protective effects of punicalagin on steroid-induced osteonecrosis in a rat model. Jt Dis Relat Surg 2026;37(x):i-xv. doi: 10.52312/jdrs.2026.2795.

ABSTRACT

Objectives: This study aims to evaluate the dose-dependent protective effects of punicalagin (PUN) in a rat model of Steroid-induced osteonecrosis of the femoral head (SONFH).

Materials and methods: Twenty-four male Wistar albino rats were randomly assigned to four groups (n = 6 per group): control, osteonecrosis (ON), ON treated with 10 mg/kg PUN, and ON treated with 40 mg/kg PUN. Osteonecrosis was induced using lipopolysaccharide and methylprednisolone. Femoral heads were evaluated using micro-computed tomography (CT), histopathological examination, and immunohistochemical analysis of cleaved caspase-3. Serum oxidative stress and antioxidant parameters including malondialdehyde (MDA), reduced glutathione (GSH), superoxide dismutase (SOD), and catalase (CAT) were measured.

Results: The primary outcome measure, the percentage of empty lacunae, was significantly higher in the ON group compared to controls (p = 0.01), showing a numerical reduction in the 40 mg/kg PUN group. Histopathological evaluation demonstrated a significant reduction in pyknotic cells in the high-dose PUN group compared to the ON group ($p < 0.05$). Furthermore, PUN treatment reduced the incidence of osteonecrosis (2/6 *vs*. 6/6; $p < 0.01$) and improved trabecular architecture. Immunohistochemical analysis showed decreased caspase-3 expression specifically in trabecular bone and adipocytes in the high-dose PUN group ($p < 0.01$), while downward trends were observed in bone marrow and endothelial cells. Micro-CT analysis confirmed a significant reduction in bone mineral density in the ON group compared to controls (p = 0.02). Regarding oxidative stress, although no statistically significant differences were observed, numerical trends toward reduced lipid peroxidation (p = 0.61) and a strong trend toward enhanced antioxidant capacity (GSH; p = 0.07) with a moderate-to-large effect size were noted.

Conclusion: Punicalagin may exert dose-dependent protective effects against SONFH in rats, primarily associated with reduced apoptotic activity and partial preservation of bone microarchitecture. While systemic oxidative stress markers show numerical improvements, the marked reduction in osteocyte apoptosis and necrotic incidence suggests that PUN represents a promising adjunctive strategy for mitigating steroid-related bone injury.

Keywords: Punicalagin; osteonecrosis; femoral head; steroid-induced osteonecrosis.

demonstrated that both the novel coronavirus disease 2019 (COVID-19) infection itself and the corticosteroids used in its treatment have contributed to an increased incidence of femoral head ON.[1] Steroid administration is a well-established risk factor for non-traumatic ON, accounting for approximately 3 to 40% of cases.[6-9] The use of these drugs may increase the risk of ON by up to 20-fold,[5] with particularly high risk observed in patients undergoing long-term treatment, particularly at daily doses exceeding 15 to 20 mg.[8,9]

The pathogenic mechanisms by which corticosteroids induce femoral head ON are multifactorial and well-documented in the literature. Corticosteroids induce vasoconstriction and elevate procoagulant factor levels, while also increasing fat cell formation and reducing bone-forming capacity. Wang et al.,[10] in a recent review, identified five major mechanisms underlying the development of steroid-induced ONFH (SONFH): altered lipid metabolism, diminished osteogenesis, compromised vascularization, apoptosis, and genetic variations. Most research supports the notion that these processes act in combination to initiate and propagate the disease.[10-13]

Punicalagin (PUN) is a polyphenol compound derived from pomegranate, known for its anti-inflammatory, antioxidant, and anticancer properties.[14,15] Various *in vitro* and *in vivo* studies have demonstrated its neuroprotective and hepatoprotective effects, primarily through antioxidant and anti-apoptotic mechanisms.[16,17] Recent research on cerebral ischemia-reperfusion injury has shown that PUN reduces neuronal degeneration. Furthermore, it has been found to inhibit apoptosis by upregulating Bcl-2 expression while downregulating Bax and caspase-3 protein levels in cerebral cortex tissue.[18-20]

To the best of our knowledge, no data are available in the literature regarding the effects of PUN on SONFH. In the present study, we, for the first time, aimed to investigate the potential protective effects of PUN against SONFH in male rats, focusing on its antioxidant and anti-apoptotic properties.

MATERIALS AND METHODS

Animals and study design

This experimental, translational study was conducted at Bağcılar Training and Research Hospital, Department of Orthopedics and Traumatology. The study protocol was approved by the institutional Ethics Committee for Animal Experiments of Bağcılar Training and Research Hospital (Date: 05.10.2020, No: 2020-25), and conducted in accordance with the Guide for the Care and Use of Laboratory Animals.

A total of 24 healthy adult male Wistar albino rats (250 to 300 g) were used in this study. Only subjects with no gross anatomical abnormalities or signs of infection upon baseline assessment were included. Exclusion criteria were defined *a priori*: animals that exhibited signs of systemic illness, developed surgical site infections, or died before the experimental endpoint. These criteria ensured that only physiologically stable animals were evaluated for ON changes. The rats were randomly divided into four groups (n = 6 per group). To minimize potential confounders, all animals were housed in cages under standard laboratory conditions (22°C, 12-h light/dark cycle) with ad libitum access to tap water and standard rodent chow. The total duration of the study was four weeks. Experimental treatments and assessments were conducted at the same time of day across groups to reduce circadian variability. Cage location and handling order were alternated to avoid systematic bias.

Experimental groups

The SONFH model was established using methods consistent with our previous study.[4] To ensure unbiased allocation, animals (n = 24) were assigned to one of the four experimental groups (n = 6 per group) using simple randomization. This allocation was performed by an investigator who was not involved in the administration of treatments or data collection to minimize potential selection bias.

While the personnel administering the treatments were aware of the group assignments due to the nature of the dosing procedures, all outcome assessments, including histological scoring, micro-computed tomography (CT) evaluation, and biochemical analyses, were performed by investigators who were strictly blinded to the group identities.

Although the personnel administering the treatments were aware of the group assignments due to the daily dosing requirements, procedural standardization was strictly maintained. Treatment sessions, handling procedures, and clinical observations were performed at the same time each day to minimize environmental and procedural bias.

The individual rat was defined as the unit of analysis for all experimental outcomes (n=6 per group). To avoid potential bias from within-rat correlation (clustering), bilateral femora were harvested and assigned to distinct evaluation modalities. Specifically, one femur from each animal was utilized for micro-CT, while the contralateral femur was processed for histopathological and immunohistochemical assessments. This ensured that each data point represented an independent biological observation from a single animal. The experimental groups were as follows (n = 6 per group):

Control Group: Rats received 1 mL/day oral phosphate-buffered saline (PBS) (Gündüz Chemical Solutions, İstanbul, Türkiye) via orogastric gavage throughout the four-week period.

ON Group: ON was induced using a combination protocol.[21] Rats received intravenous injections of lipopolysaccharide (LPS, Escherichia coli O55:B5, Sigma, St. Louis, MO, USA) at 20 µg/kg on Days 0 and 1, followed by intramuscular injections of methylprednisolone sodium succinate (Prednol®, Mustafa Nevzat Pharmaceuticals, Istanbul, Türkiye) at 40 mg/kg on Days 3, 4, and 5. Rats also received daily oral PBS (1 mL) until sacrifice.

ON + 10 mg/kg PUN: ON was induced as in ON Group. Simultaneously, rats received 10 mg/kg/day PUN (Sigma Chemical, Louis, MO, USA) by orogastric gavage throughout the four-week period.

ON + 40 mg/kg PUN: ON was induced as in ON Group. Simultaneously, rats received 40 mg/kg/day PUN via orogastric gavage for four weeks.

Punicalagin was freshly prepared daily in PBS solution.[22] At the end of the study, all rats were sacrificed under general anesthesia. Intracardiac blood samples were collected for biochemical analysis, followed by euthanasia via cervical dislocation.

Micro-CT evaluation

After sacrifice, bilateral femora were harvested and preserved in 10% buffered formalin. To maintain the individual rat as the independent unit of analysis (n = 6 per group) and avoid pseudoreplication, one femur from each animal was randomly assigned for radiological assessment. Micro-CT was performed to evaluate structural parameters including bone mineral density (BMD), bone volume/total volume fraction (BV/TV), trabecular thickness (Tb.Th), trabecular number (Tb.N), trabecular separation (Tb.Sp), structure model index (SMI), and bone surface-to-volume ratio (BS/BV).

Histopathological and immunohistochemical analyses

To ensure the independence of observations, the contralateral femur from each rat, which were not used for micro-CT imaging previously, was utilized for histopathological and immunohistochemical assessments. These specimens were decalcified in 10% formic acid and embedded in paraffin blocks. For each animal, a minimum of five longitudinal sections (3 to 4 µm in thickness) were prepared from the femoral head, and at least five representative fields per section were evaluated under light microscopy. All histopathological and immunohistochemical assessments were performed by a single experienced pathologist who was blinded to the group assignments. As all assessments were performed by a single pathologist, formal inter-rater and intra-rater reliability analyses were not conducted; however, all scoring decisions were made in strict accordance with the pre-defined histopathological criteria described below.

The sections were stained with hematoxylin-eosin (H&E) or Masson's trichrome for histopathological evaluation. Parameters assessed included ON, femoral head structural abnormality, trabecular integrity, osteocyte viability, and bone marrow morphology. Femoral head ON and associated structural anomalies were evaluated based on established histopathological criteria. An ON focus was defined by the presence of three or more of the following features in the same region: (1) empty or irregular osteocytic lacunae, (2) pyknotic or shrunken osteocyte nuclei, (3) disruption or fragmentation of trabecular bone structure, and (4) bone marrow alterations such as fat cell hypertrophy, hemorrhage, thrombosis, or hematopoietic cell necrosis. These criteria were used to determine the presence and extent of femoral head anomalies across the experimental groups.

For immunohistochemical analysis, cleaved caspase-3 expression was assessed in the adipocytes, trabeculae, bone marrow, and endothelial cells using a standard avidin-biotin-peroxidase complex method according to the literature.[23] Immunohistochemical staining was semi-quantitatively evaluated using the H-score method, which combines staining intensity and the percentage of positive cells, calculated by multiplying the proportion of cells at each intensity

level by the corresponding intensity score, yielding a total score ranging from 0 to 300.

Biochemical analysis

Serum samples were centrifuged at 3,000 rpm for 10 min and stored at –80°C until analysis. Oxidative stress markers, including malondialdehyde (MDA) (Rat MDA ELISA Kit, Mybiosource), reduced glutathione (GSH) (Rat Reduced glutathione ELISA Kit, Mybiosource), superoxide dismutase (SOD) (Rat Superoxide Dismutase ELISA Kit, Mybiosource), and catalase (CAT) (Rat Catalase ELISA Kit, Mybiosource), were measured using commercial enzyme-linked immunosorbent assay (ELISA) kits.

Outcome measures

The outcome measures assessed in this study included:

- Histopathological evidence of ON, such as empty lacunae, pyknotic nuclei, and trabecular bone disorganization, evaluated via H&E staining
- Microstructural bone parameters obtained by micro-CT, including Tb.N, Tb.Th, BV/TV, and Tb.Sp
- Immunohistochemical reactivity of caspase-3 in femoral tissues
- Oxidative stress/antioxidant biomarkers, including serum levels of MDA, GSH, SOD and CAT.

The primary outcome measure for the purpose of sample size determination was the percentage of empty lacunae, as a quantitative histopathological index of osteocyte loss that directly reflects the extent of bone tissue necrosis and correlates with treatment efficacy. This endpoint was selected based on its sensitivity and reproducibility in previous ON models.

Statistical analysis

No formal *a priori* sample size calculation was conducted. The present study was designed as an exploratory (pilot) study to investigate the effects of PUN on SONFH, with a sample size of n = 6 per group chosen based on similar experimental rat models in the literature, as well as ethical principles of animal research.[6,16] This group size was shown to be sufficient to detect histological changes in bone tissue in prior studies.[23] To retrospectively evaluate the adequacy of the sample size, a *post-hoc* power analysis was performed using the G*Power version 3.1 software (Heinrich Heine University, Düsseldorf, Düsseldorf, Germany), based on the primary outcome measure of empty lacunae percentage. Using a one-way analysis of variance (ANOVA) model with four groups and a total sample size of 24, an observed effect size of f = 1.30 and a significance level of $\alpha = 0.05$, the achieved statistical power was calculated as 99.9% ($1\text{-}\beta = 0.999$). These results confirm that the sample size employed was sufficient to detect statistically meaningful differences for the primary outcome variable.

Statistical analysis was performed using the SPSS version 26.0 software (IBM Corp., Armonk, NY, USA). Given the small sample size (n = 6 per group), normality testing (Shapiro-Wilk) was considered to have insufficient statistical power to reliably detect departures from normality. Therefore, non-parametric methods were selected *a priori* for all group comparisons, regardless of the results of formal normality testing. Comparisons between groups were performed using the Kruskal-Wallis test followed by Dunn's multiple comparisons test. Descriptive data were presented in median (min-max) or number and frequency, where applicable. For Kruskal-Wallis comparisons, epsilon-squared (ε^2) was calculated and reported as a measure of effect size, with values of 0.01, 0.06, and 0.14 interpreted as small, moderate, and large effects, respectively. For Fisher's exact test analyses, effect size was directly interpreted from the reported group-wise proportions (X/N). No additional correction for multiple testing (Holm or Benjamini-Hochberg) was applied beyond the Dunn *post-hoc* procedure, given the exploratory nature of this study. All reported p-values should therefore be interpreted in this context. A p value of <0.05 was considered statistically significant.

RESULTS

All animals (n = 6 per group) initially assigned to each experimental group completed the study and were included in the analysis.

Histopathological findings

As the primary outcome measure of this study, the percentage of empty lacunae was evaluated histopathological in femoral head sections stained with H&E and Masson's trichrome and revealed significant differences between the experimental groups (Figures 1 and 2). In the ON group, extensive ON areas were identified based on established histological criteria, including a high prevalence of empty osteocytic lacunae, increased numbers

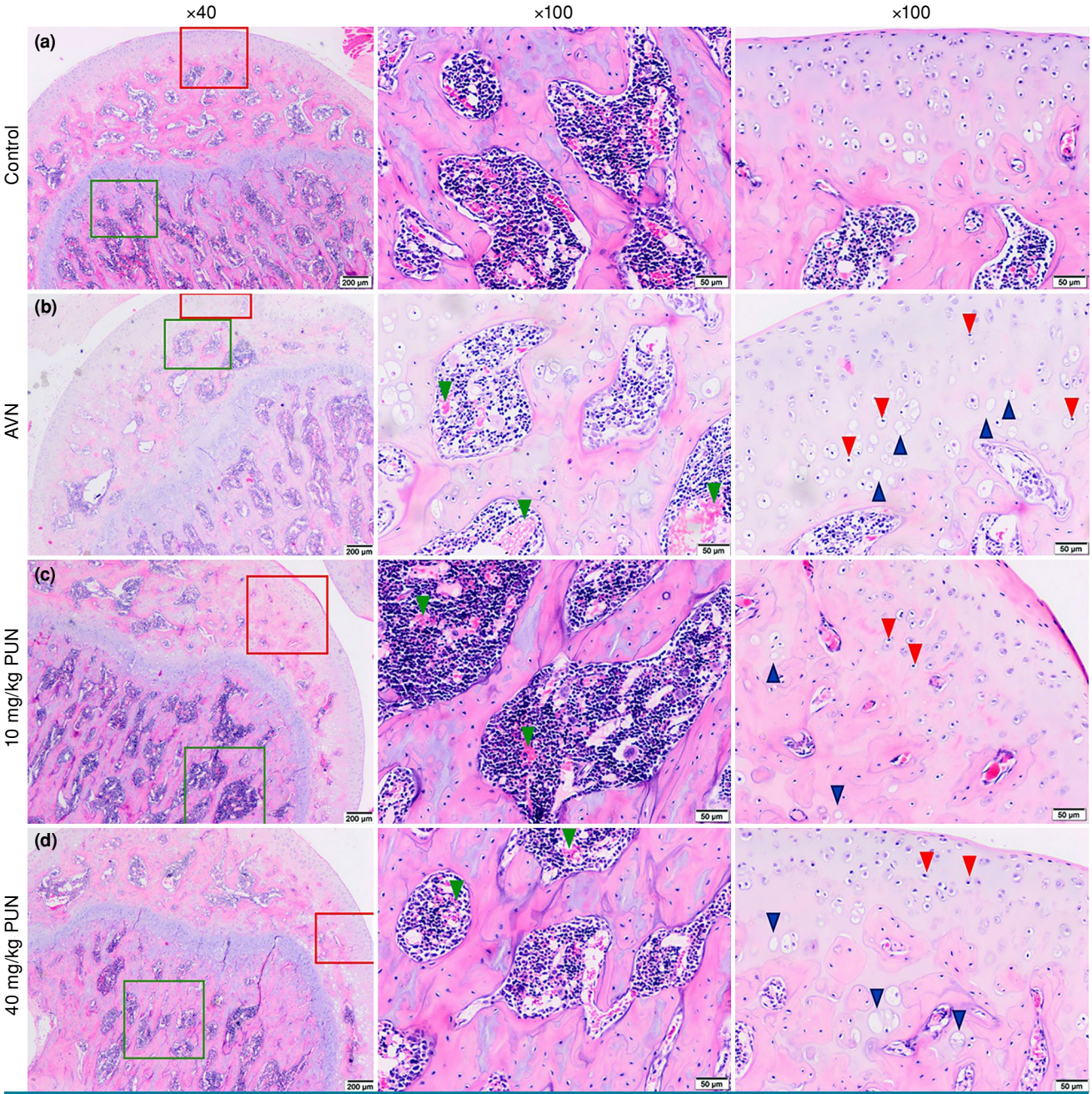

FIGURE 1. Hematoxylin and eosin-stained sections of rat femoral heads showing histopathological changes across study groups (n = 6 per group). Left column: low-magnification overview (scale bar = 200 μm); middle and right columns: high-magnification images of boxed regions indicated in the low-magnification panels (scale bar = 50 μm). Red boxes indicate regions enlarged in the middle column; green boxes indicate regions enlarged in the right column. **(a)** Control group showing normal trabecular bone structure and viable osteocytes with intact lacunae. **(b)** ON group exhibiting extensive osteonecrosis with disorganized trabecular architecture. **(c)** 10 mg/kg PUN group showing partial preservation of bone structure and reduced necrotic areas. **(d)** 40 mg/kg PUN group demonstrating improved trabecular architecture with decreased osteonecrosis. In high-magnification panels: blue arrowheads indicate empty osteocytic lacunae; red arrowheads indicate pyknotic osteocyte nuclei; green arrowheads indicate bone marrow abnormalities including adipocyte hypertrophy and hematopoietic changes.

ON, osteonecrosis; PUN, Punicalagin.

of pyknotic nuclei, and fragmented trabecular bone architecture. Osteonecrosis was defined histologically by the presence of at least three of the following features: empty lacunae, pyknotic nuclei, loss of trabecular continuity, and bone marrow abnormalities. These pathological features were

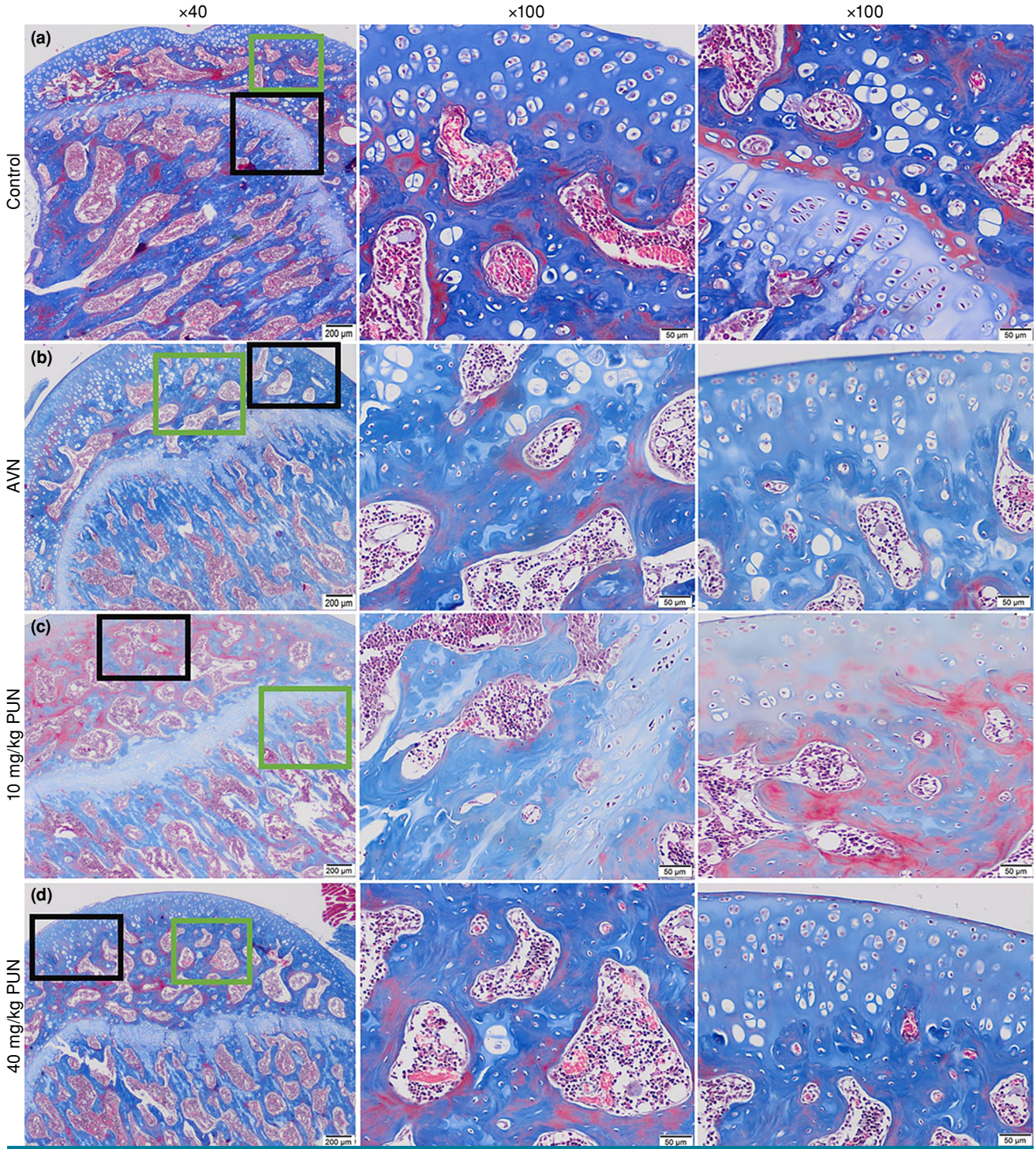

FIGURE 2. Masson's trichrome staining of femoral head sections illustrating bone matrix integrity and collagen distribution. Left column: low-magnification overview (scale bar = 200 μm); middle and right columns: high-magnification images of boxed regions (scale bar = 50 μm). Green boxes indicate regions enlarged in the middle column; black boxes indicate regions enlarged in the right column. **(a)** Control group with regular and continuous collagen deposition within trabeculae. **(b)** ON group showing disrupted and disorganized collagen matrix with structural fragmentation and loss of trabecular continuity. **(c)** 10 mg/kg PUN group demonstrating partial collagen preservation. **(d)** 40 mg/kg PUN group exhibiting improved collagen integrity and trabecular organization compared to the ON group.

ON, osteonecrosis; PUN, punicalagin; AVN, avascular necrosis ON group.

TABLE I
Comparison of histopathological findings of femoral head sections according to groups (n=6) of the ON model

	Control	ON	10 mg/kg PUN	40 mg/kg PUN	*p*
Categorical outcomes			X/N		
Osteonecrosis	0/6	6/6	4/6	2/6	**< 0.01**
Femur head structural abnormality	0/6	6/6	4/6	2/6	**< 0.01**
Bone trabeculae					
Regular	6/6	0/6	0/6	4/6	**< 0.01**
Partially regular	0/6	2/6	2/6	0/6	0.19
Irregular	0/6	4/6	4/6	2/6	0.06
Thin	0/6	4/6	4/6	2/6	0.06
Intermittent/Space	0/6	4/6	4/6	2/6	0.06
Fractured	0/6	0/6	0/6	0/6	-
Granulation	0/6	3/6	1/6	2/6	0.21
Fibrosis	0/6	5/6	3/6	2/6	**0.03**
Osteocytes					
Marked	6/6	2/6	2/6	4/6	0.06
Sparse	0/6	4/6	4/6	2/6	0.06
Bone marrow					
Normal	5/6	0/6	0/6	0/6	**< 0.01**
Increased adipocyte #	1/6	6/6	6/6	6/6	**< 0.01**
Large adipocytes	0/6	6/6	4/6	2/6	**< 0.01**
Hemorrhage	0/6	6/6	4/6	6/6	**< 0.01**
Thrombus	0/6	5/6	4/6	6/6	**< 0.01**
Macrophage	2/6	5/6	4/6	6/6	0.07
Increased HC #	0/6	0/6	0/6	4/6	**< 0.01**
Decreased HC #	0/6	6/6	3/6	2/6	**< 0.01**
HC necrosis	0/6	6/6	3/6	4/6	**< 0.01**

Continuous outcomes	n	Median	Min-Max	*p*	Post Hoc	Effect size (ε^2)
Pyknotic cell (%)						
Control[1]	6	13.3	0 to 26.7	**0.03***	1 < 2, 1 < 3, 2 > 4	0.46
ON[2]	6	41.5	24.1 to 64.0			
10 mg/kg PUN[3]	6	31.0	15.3 to 52.6			
40 mg/kg PUN[4]	6	10.8	4.3 to 33.3			
Empty lacunae (%)						
Control[1]	6	6.7	2.3 to 34.3	**0.01****	1 < 2, 1 < 3, 1 < 4	0.63
ON[2]	6	58.7	50.0 to 75.3			
10 mg/kg PUN[3]	6	47.8	31.9 to 69.6			
40 mg/kg PUN[4]	6	34.2	30.1 to 45.1			
Vascular thrombosis (%)						
Control[1]	6	18.2	0 to 45.5	**0.01****	1 < 2, 1 < 3, 1 < 4	0.61
ON[2]	6	87.7	66.7 to 100			
10 mg/kg PUN[3]	6	69.6	42.9 to 92.3			
40 mg/kg PUN[4]	6	40.0	36.8 to 55.6			

ON, osteonecrosis; PUN, punicalagin; HC, hematopoietic cells; X/N, number of animal with pathology/total number of animals; 1, Control group; 2, ON group; 3, 10 mg/kg PUN group; 4, 40 mg/kg PUN group. Categorical data (Osteonecrosis, Structural Abnormality, etc.) were analyzed using Fisher's Exact test. Continuous data (Empty lacunae %, etc.) were analyzed using Kruskall Wallis followed by Dunn's post-hoc test. $P < 0.05$ was considered statistically significant. * $p < 0.05$; ** $p < 0.01$.

accompanied by prominent marrow alterations, including adipocyte hypertrophy, hemorrhage, and hematopoietic cell necrosis.

Masson's trichrome staining highlighted disrupted collagen distribution and trabecular fragmentation in the ON group, with notable loss

of structural integrity (Figure 2). Conversely, rats treated with PUN demonstrated dose-dependent improvements in bone microarchitecture. In the 40 mg/kg PUN group, trabeculae appeared more continuous with preserved osteocyte morphology. Categorical analysis confirmed these observations: the incidence of ON and structural abnormalities was 100% (6/6) in the ON group, while it was significantly lower in the 40 mg/kg PUN group (2/6; $p < 0.01$) (Table I).

Quantitative analysis revealed that the percentage of pyknotic cells was significantly reduced in the 40 mg/kg PUN group (median: 10.8%) compared to the ON group (median: 41.5%; $p < 0.05$). For the primary endpoint, the median percentage of empty lacunae in the ON group (58.7%) was substantially higher than in controls (6.7%), while treatment with 40 mg/kg PUN resulted in a numerical reduction to 34.2%. Additionally, bone marrow thrombosis and adipocyte enlargement, which were prominent in the ON group, were notably ameliorated by PUN, particularly at the higher dose (Figures 1 and 2).

Immunohistochemical analysis

Immunohistochemical staining for cleaved caspase-3 was performed on the contralateral femoral heads to evaluate apoptotic activity across n = 6 independent biological replicates per group (Figure 3). The semiquantitative H-score results, presented as minimum-maximum (median), revealed significant differences in apoptotic expression across all four compartments of the femoral head (Table II).

In the adipocyte and trabecular compartments, steroid induction (ON group) led to a marked increase in caspase-3 immunopositivity compared to the control group ($p < 0.01$). High-dose PUN (40 mg/kg) significantly attenuated this apoptotic response, as median H-scores in the 40 mg/kg PUN group were significantly lower than both the ON and 10 mg/kg PUN groups ($p < 0.01$ for adipocytes and trabecula, according to Dunn's *post-hoc* test).

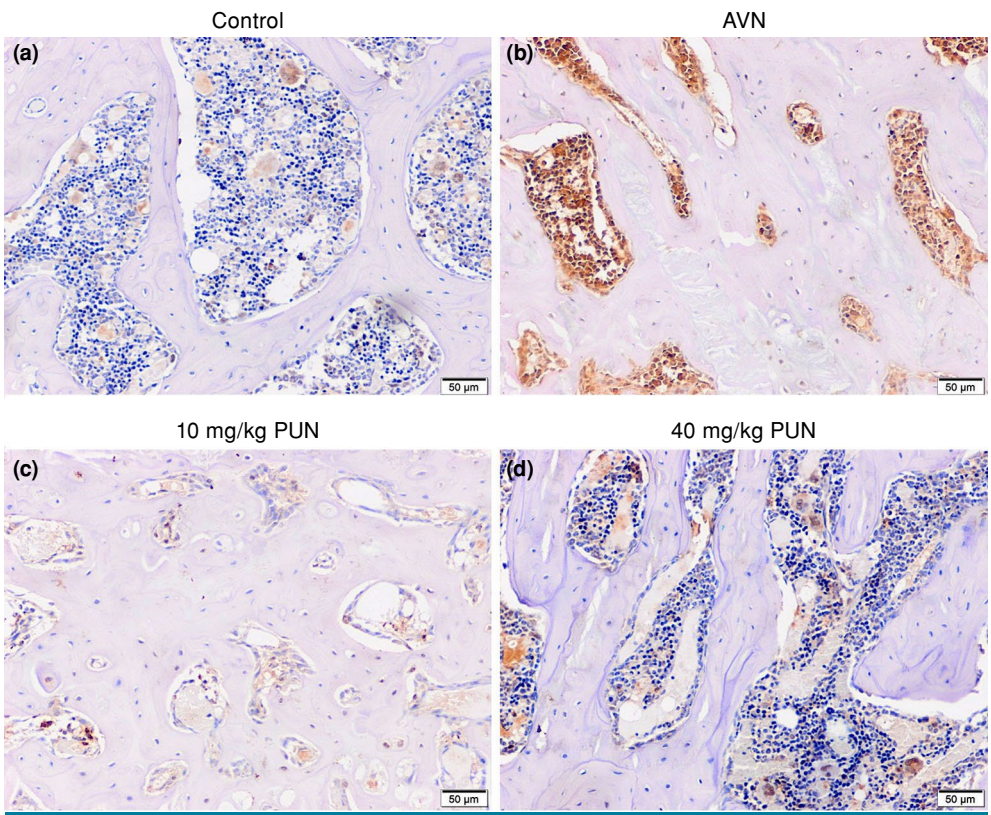

FIGURE 3. Representative photomicrographs of immunohistochemical staining for cleaved caspase-3 in rat femoral head sections indicating apoptotic activity from **(a)** control, **(b)** ON, **(c)** 10 mg/kg PUN, and **(d)** 40 mg/kg PUN groups. Strong cytoplasmic immunopositivity is evident in bone marrow, trabeculae, and endothelial cells in the ON group, with progressive reduction in PUN-treated groups. Original magnification: ×200 (scale bar = 50 µm).
AVN, avascular necrosis ON group.

Notably, the effect size for these compartments was large ($\varepsilon^2 = 0.59$ and 0.66, respectively), indicating a robust protective effect of PUN on osteocyte and adipocyte viability.

Significant group differences were also observed in the bone marrow ($p < 0.05$) and endothelia ($p < 0.01$). In the bone marrow, *post-hoc* analysis confirmed that caspase-3 expression was

TABLE II
Comparison of immunohistochemical and biochemical findings of femoral head sections according to groups (n = 6) of the ON model

Immunohistochemical findings	n	Median	Min-Max	*p*	Post Hoc	Effect size (ε^2)
Adipocytes						
Control[1]	6	37.5	0 to 75	**<0.01****	1 < 2; 1 < 3; 2 > 4; 3 > 4	0.59
ON[2]	6	150	100 to 200			
10 mg/kg PUN[3]	6	150	100 to 200			
40 mg/kg PUN[4]	6	50	25 to 150			
Bone marrow						
Control[1]	6	100	50 to 150	**0.01***	1 < 2; 1 < 3	0.41
ON[2]	6	287.5	200 to 300			
10 mg/kg PUN[3]	6	287.5	200 to 300			
40 mg/kg PUN[4]	6	175	50 to 300			
Trabecula						
Control[1]	6	0	0 to 25	**<0.01****	1 < 2; 1 < 3; 2 > 4; 3 > 4	0.66
ON[2]	6	100	25 to 150			
10 mg/kg PUN[3]	6	100	25 to 150			
40 mg/kg PUN[4]	6	0	0 to 50			
Endothelia						
Control[1]	6	25	0 to 100	**0.01****	1 < 2; 1 < 3; 1 < 4	0.43
ON[2]	6	225	50 to 300			
10 mg/kg PUN[3]	6	225	50 to 300			
40 mg/kg PUN[4]	6	175	50 to 250			
MDA (nmol/L)						
Control[1]	6	51.16	13.89 to 87.58	0.61	-	0.00
ON[2]	6	37.5	9.17 to 76.29			
10 mg/kg PUN[3]	6	37.05	21.27 to 60.72			
40 mg/kg PUN[4]	6	29.44	15.84 to 42.27			
GSH (mg/L)						
Control[1]	6	340.84	196.49 to 438.62	0.07	-	0.21
ON[2]	6	290.32	246.48 to 400.44			
10 mg/kg PUN[3]	6	325.34	296.42 to 477.68			
40 mg/kg PUN[4]	6	451.05	430.82 to 471.81			
SOD (U/mL)						
Control[1]	6	295	264 to 310	0.28	-	0.04
ON[2]	6	291.5	264 to 316			
10 mg/kg PUN[3]	6	300.5	296 to 306			
40 mg/kg PUN[4]	6	311	299 to 312			
CAT (U/mL)						
Control[1]	6	128.35	47.4 to 442.6	0.88	-	0.00
ON[2]	6	245.35	29.9 to 462.1			
10 mg/kg PUN[3]	6	121.5	20.1 to 332.1			
40 mg/kg PUN[4]	6	260	77.3 to 268.4			

ON, osteonecrosis; PUN, punicalagin; MDA, malondialdehyde; GSH, glutathione; SOD, superoxide dismutase, CAT, catalase; 1, Control group; 2, ON group; 3, 10 mg/kg PUN group; 4, 40 mg/kg PUN group. Data were analyzed using Kruskall Wallis followed by Dunn's post-hoc test. * $p < 0.05$ and ** $p < 0.01$ were considered statistically significant.

significantly higher in the ON and 10 mg/kg PUN groups relative to controls, while the 40 mg/kg group showed a median value (175) lower than the ON group (287.5), although this did not reach statistical significance in the pairwise comparison. Similarly, in the endothelial compartment, all treatment and induction groups remained significantly higher than the control group, suggesting that while PUN treatment showed a downward trend in endothelial apoptosis (median

TABLE III
Comparison of radiological findings of femoral head sections according to groups (n = 6) of the ON model

	n	Median	Min-Max	*p*	Post Hoc	Effect size (ε^2)
BMD						
Control[1]	6	1.15	0.98 to 1.25	0.02*	1>2; 1>3; 1>4	0.42
ON[2]	6	1.03	0.9 to 1.07			
10 mg/kg PUN[3]	6	1	0.83 to 1.12			
40 mg/kg PUN[4]	6	0.93	0.85 to 0.96			
BV / TV (%)						
Control[1]	6	89.43	86.69 to 93.99	0.36		0.05
ON[2]	6	88.29	82.99 to 92.16			
10 mg/kg PUN[3]	6	89.59	72.28 to 95.91			
40 mg/kg PUN[4]	6	85.98	76.86 to 88.03			
BS / BV (mm^{-1})						
Control[1]	6	7.86	6.76 to 8.72	0.21		0.09
ON[2]	6	8.44	7.38 to 9.74			
10 mg/kg PUN[3]	6	7.83	5.69 to 12.03			
40 mg/kg PUN[4]	6	9.14	8.72 to 10.81			
Tb. Th (mm)						
Control[1]	6	0.29	0.24 to 0.31	0.21		0.09
ON[2]	6	0.28	0.22 to 0.32			
10 mg/kg PUN[3]	6	0.27	0.17 to 0.41			
40 mg/kg PUN[4]	6	0.24	0.2 to 0.24			
Tb. N (mm^{-1})						
Control[1]	6	3.08	2.91 to 3.65	0.18		0.10
ON[2]	6	3.14	2.87 to 3.72			
10 mg/kg PUN[3]	6	3.28	2.27 to 4.21			
40 mg/kg PUN[4]	6	3.74	3.61 to 3.9			
Porosity (%)						
Control[1]	6	10.57	6.01 to 13.31	0.36		0.05
ON[2]	6	11.71	7.84 to 17.01			
10 mg/kg PUN[3]	6	10.41	4.09 to 27.72			
40 mg/kg PUN[4]	6	14.02	11.97 to 23.14			
Tb. Sp (mm^{-1})						
Control[1]	6	0.11	0.08 to 0.12	0.36		0.05
ON[2]	6	0.11	0.1 to 0.12			
10 mg/kg PUN[3]	6	0.11	0.08 to 0.13			
40 mg/kg PUN[4]	6	0.11	0.1 to 0.14			
Tb.Pf. (mm^{-1})						
Control[1]	6	–10.01	–12.35 to –9.44	0.36		0.05
ON[2]	6	–8.84	–9.52 to –8.67			
10 mg/kg PUN[3]	6	–9.39	–10.47 to –6.9			
40 mg/kg PUN[4]	6	–10.07	–12.41 to –6.88			

ON, osteonecrosis; BMD, bone mineral density; PUN, punicalagin; BV / TV, bone volume / total volume; BS / BV, bone surface area / bone volume; Tb. Th, trabecular thickness; Tb. N., trabecular number, Tb. Sp, trabecular space; Tb. Pf., trabecular bone model factor; 1, Control group; 2, ON group; 3, 10 mg/kg PUN group; 4, 40 mg/kg PUN group. Data were analyzed using Kruskall Wallis followed by Dunn's post-hoc test. * $p < 0.05$ were considered statistically significant.

175 *vs.* 225), the protection was partial at the doses evaluated.

These findings suggest that PUN treatment attenuates caspase-3-mediated apoptosis in osseous, marrow, adipocytic, and vascular components of the femoral head, with a more evident protective effect at higher doses. However, the §elevated endothelial H-scores persisting even in the 40 mg/kg PUN group suggest that endothelial apoptosis was only partially mitigated, which may have implications for vascular integrity and microcirculatory function in SONFH and is discussed further below.

Oxidative stress and antioxidant parameters

Serum biochemical analysis, performed on samples from n = 6 independent replicates per group, evaluated systemic oxidative stress and antioxidant capacity. As detailed in Table II, no statistically significant differences were found in serum MDA levels across the experimental groups (p = 0.61), although the 40 mg/kg PUN group displayed a lower median value (29.44 nmol/L) compared to the ON group (37.5 nmol/L). Regarding antioxidant status, GSH levels exhibited a trend toward dose-dependent enhancement, with the 40 mg/kg PUN group showing a higher median concentration (451.05 mg/L) relative to the ON group (290.32 mg/L). While this did not reach the conventional threshold for statistical significance (p = 0.07), the calculated effect size (ε^2 = 0.21) suggests a moderate-to-large biological impact of high-dose PUN on antioxidant reserves. Similarly, serum SOD and CAT levels did not significantly differ between the experimental groups (p = 0.28 and p = 0.88, respectively).

Radiological evaluation

Table III summarizes the radiological findings of the femoral head sections across the experimental groups. To ensure the independence of observations and to avoid potential bias from within-subject correlation (clustering), micro-CT assessments were performed on one randomly selected femur per animal, representing six independent biological replicates per group (n = 6). A significant inter-group difference was identified in BMD (p = 0.02) with a substantial effect size (ε^2 = 0.42). Dunn's *post-hoc* analysis revealed that the median BMD in the control group (1.15 g/cm^3) was significantly higher than in the ON group (1.03 g/cm^3) and both PUN-treated groups ($p < 0.05$).

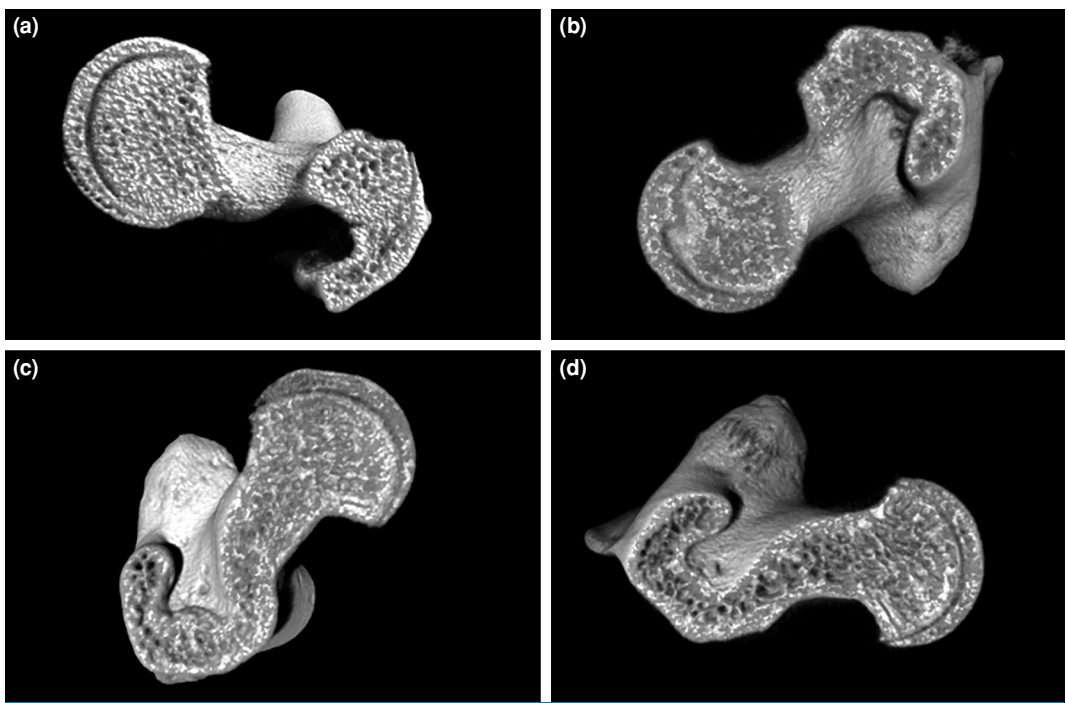

FIGURE 4. Representative axial micro-computed tomography (micro-CT) images of the femoral head in the study groups. **(a)** Control group, **(b)** osteonecrosis group, **(c)** punicalagin 10 mg group, and **(d)** punicalagin 40 mg group.
CT, computed tomography.

Other micro-architectural parameters, including BV/TV, BS/BV, Tb.Th, and porosity, did not reach statistical significance ($p > 0.05$; Table III. Nevertheless, numerical trends toward improved bone structure were observed in the 40 mg/kg PUN group, such as an increase in the median Tb.N (3.74 mm^{-1}) compared to the ON group (3.14 mm^{-1}) (Figure 4, Table III). While steroid administration significantly reduced BMD, the structural trabecular alterations were only partially mitigated by PUN treatment within the study's timeframe.

DISCUSSION

In the present study, we investigated the potential protective effects of PUN against SONFH in male rats, focusing on its antioxidant and anti-apoptotic properties. The rat model of SONFH was selected due to its well-established histopathological and radiological resemblance to human ON. Glucocorticoid administration in rats reliably induced ON lesions through mechanisms similar to those observed in humans, including vascular compromise, oxidative stress, and impaired bone remodeling. This model allowed for the controlled evaluation of therapeutic agents and their effects on bone microarchitecture and cellular integrity. Punicalagin exerted a dose-dependent protective effect against SONFH in this model. The micro-CT findings revealed that PUN reduced the steroid-induced reduction in BMD, while histopathological analyses showed marked improvements in trabecular continuity, osteocyte viability, and bone marrow architecture, particularly at the higher dose. In parallel, immunohistochemical findings demonstrated a significant reduction in cleaved caspase-3 expression in both bone and endothelial cells, suggesting attenuation of apoptosis. These cellular benefits were accompanied by numerical improvements in oxidative stress markers and a near-significant enhancement of antioxidant capacity. These findings suggest that PUN may protect against SONFH by preserving bone microarchitecture and reducing oxidative stress-associated apoptotic damage.

In addition, micro-CT analysis confirmed that steroid administration resulted in a significant decline in BMD, consistent with previous experimental and clinical observations in early-stage ON.[24] Although several trabecular parameters did not reach statistical significance, the 40 mg/kg PUN-treated group exhibited numerical trends toward improved bone structure, such as an increase in median Tb.N compared to the ON group. Of note, these findings should be interpreted with caution, as the relatively small sample size may have resulted in insufficient statistical power to detect subtle changes in bone microarchitecture. Future studies with larger sample sizes are warranted to definitively confirm these radiological trends. These trends may suggest a potential effect; however, they should be interpreted cautiously due to limited statistical power. Nevertheless, such observations may reflect partial preservation of bone microarchitecture that could translate into delayed femoral head structural abnormality and collapse.[18,24,25] Similar microstructural improvements have been reported with other osteoprotective agents in experimental SONFH models, supporting the relevance of these findings.[21,26]

Histopathological evaluation further substantiated the protective role of PUN. Animals in the ON group exhibited classic features of femoral head necrosis, including extensive empty osteocytic lacunae, pyknotic nuclei, disrupted trabecular architecture, and bone marrow abnormalities such as adipocyte hypertrophy and vascular thrombosis. In contrast, PUN treatment supporting reduced the incidence and severity of these pathological features in a dose-dependent manner. The reduction in empty lacunae and pyknotic osteocytes suggests improved osteocyte survival, which is critical for maintaining bone integrity and mechanotransduction within the femoral head.

Apoptosis plays a central role in the pathogenesis of steroid-induced ON, affecting both osteocytes and endothelial cells and thereby compromising bone viability and microcirculation.[27] In the present study, cleaved caspase-3 expression was significantly increased in trabecular bone, bone marrow, and endothelial cells following steroid exposure. The numerical attenuation of endothelial caspase-3 expression observed in PUN-treated groups warrants specific discussion in the context of SONFH pathophysiology. Endothelial apoptosis plays a central role in the microvascular dysfunction that underlies steroid-induced ON, as loss of endothelial integrity compromises sinusoidal blood flow, promotes intravascular thrombosis, and ultimately leads to ischemic necrosis of bone tissue.[16] The persistence of relatively elevated endothelial H-scores in the 40 mg/kg PUN group, which did not reach statistical significance compared to the ON group in *post-hoc* analysis, suggests that the anti-apoptotic effects of PUN, while statistically significant in trabecular

and adipocytic compartments, may be insufficient to fully restore endothelial homeostasis at the doses tested. This could reflect the particularly high susceptibility of endothelial cells to glucocorticoid-induced oxidative stress and apoptosis, which may require higher doses, prolonged treatment, or adjunctive vascular-protective strategies to achieve complete protection. These findings align with previous experimental studies demonstrating that PUN can attenuate apoptosis in various tissues under conditions of oxidative or ischemic stress.[28-30] Alternatively, structural vascular remodeling initiated during the early phases of steroid exposure may not be fully reversible within the four-week treatment window of this study. The present findings support endothelial protection as a potential therapeutic target in SONFH and suggest that future studies should investigate higher doses of PUN, longer treatment durations, and combination strategies targeting both oxidative stress and endothelial apoptosis pathways.

Oxidative stress is another key contributor to steroid-induced bone damage.[31] Elevated lipid peroxidation and impaired antioxidant defenses promote cellular injury and apoptosis within the femoral head. In our model, although steroid administration led to a numerical increase in serum MDA levels and a decrease in antioxidant capacity, these inter-group differences did not reach statistical significance. However, PUN treatment demonstrated a downward numerical trend in MDA levels, suggesting a potential mitigating effect. Importantly, GSH levels exhibited a strong trend toward dose-dependent enhancement, with a moderate-to-large effect size ($\varepsilon^2 = 0.21$) in the high-dose group. Previous experimental studies have shown that PUN reduces oxidative stress through enhancement of endogenous antioxidant systems, providing a plausible biological explanation for the protective effects observed in the present study.[29,30] The protective effects of PUN observed in our study are consistent with the broader literature emphasizing the role of antioxidant-rich natural compounds in mitigating musculoskeletal degeneration. In their study, Erturk et al.[32] recently demonstrated that extra virgin olive oil significantly alleviates articular cartilage damage by reducing oxidative stress-mediated lipid peroxidation and ox-LDL levels in a rat model. These findings suggest that, similar to other potent natural antioxidants, PUN may preserve bone and joint integrity by countering the systemic and local oxidative drive that characterizes steroid-induced damage.

Beyond steroid-induced ON models, PUN has also been shown to attenuate inflammatory bone loss in other experimental settings. In an *in vivo* model of aseptic osteolysis, PUN significantly reduced inflammatory bone resorption and preserved bone integrity, highlighting its broader osteoprotective potential.[33] These findings suggest that the beneficial effects of PUN may extend across different pathological bone microenvironments characterized by inflammation, oxidative stress, and increased cell death.

While mechanistic pathways such as AMPK or NF-κB signaling have been implicated in previous studies, these pathways were not directly assessed in the current work and therefore cannot be conclusively addressed.[34] Nevertheless, the consistency between our *in vivo* findings and prior mechanistic studies supports the biological plausibility of PUN as a protective agent against steroid-induced ON. To ensure experimental transparency in line with ARRIVE guidelines, simple randomization was performed by an independent investigator to minimize selection bias. While treatment administration was not blinded due to dosing requirements, all outcome assessments were conducted by strictly blinded investigators to mitigate observer bias. Furthermore, procedural standardization, including identical housing and synchronized care, was rigorously maintained to ensure the reproducibility of our findings. Several limitations should be acknowledged. In the present study, the suppression of apoptotic activity by PUN was assessed solely through cleaved caspase-3 immunohistochemistry. While this marker is a reliable indicator of the execution phase of apoptosis, our findings should be interpreted as associative rather than mechanistically definitive. We acknowledge that additional molecular markers, such as the Bcl-2/Bax ratio, which regulates the mitochondrial apoptotic pathway, or the Nrf2/HO-1 signaling pathway, which links antioxidant defenses to cell survival, were not evaluated. Therefore, while our results demonstrate a strong association between PUN treatment and reduced apoptosis in the femoral head, the precise molecular orchestration underlying this effect remains to be elucidated in future studies incorporating a broader range of molecular markers. Another limitation of the histopathological assessment is that all evaluations were performed by a single pathologist; formal inter-rater reliability analysis

was, therefore, not possible. The relatively modest sample size (n = 6 per group) represents a notable limitation of this study. Larger sample sizes are warranted in future studies to further strengthen the pharmacological conclusions. The study was conducted over a relatively short experimental period and did not include direct molecular pathway analyses. Additionally, the absence of *in vitro* experiments limits detailed mechanistic interpretation. Future studies incorporating longer follow-up periods, molecular signaling assessments, and complementary *in vitro* models would help to further elucidate the precise mechanisms underlying PUN's osteoprotective effects. As apoptosis was assessed solely through cleaved caspase-3 expression, the current findings remain primarily associative and do not establish a definitive mechanistic pathway underlying the observed effects.

In conclusion, this study provides preclinical evidence that PUN may confer dose-dependent protective effects against SONFH in rats. This protection is primarily associated with a significant reduction in apoptotic activity and improved histopathological outcomes, including a lower incidence of ON. While systemic oxidative stress markers and radiological bone microarchitecture show numerical improvements and trends toward preservation, the marked reduction in osteocyte necrosis suggests that PUN is a potential candidate for further investigation for mitigating steroid-related bone injury. These results support further investigation of PUN in advanced preclinical models to definitively elucidate the specific molecular pathways involved and to validate these findings for potential clinical applications in high-risk populations.

Acknowledgments: The authors would like to thank the Bagcilar Training and Research Hospital Experimental Research and Skill Development Center for providing infrastructure and technical support for the experimental procedures. The authors also gratefully acknowledge Büşra Yaprak Bayrak (Department of Pathology, Faculty of Medicine, Kocaeli University, Kocaeli, Türkiye) for her valuable contributions to the pathological evaluations.

Data Sharing Statement: The data that support the findings of this study are available from the corresponding author upon reasonable request.

Author Contributions: M.U.: Idea/concept, writing the article; O.B.: Data collection and processing; Y.Ö.: Analysis and interpretation; E.C.B.: Materials, references; Y.G.: Critical Review, data collection; A.A.: Literature review; M.F.D.: Critical review, writing the article; E.A.: Control/supervision.

Conflict of Interest: The authors declared no conflicts of interest with respect to the authorship and/or publication of this article.

Funding: This work was funded by Revolving Fund Budget Research and Development Expenses Account of Bagcilar Education and Research Hospital, Istanbul, Turkey (22.01.2021; No. 2021/1).

AI Disclosure: The authors declare that artificial intelligence (AI) tools were not used, or were used solely for language editing, and had no role in data analysis, interpretation, or the formulation of conclusions. All scientific content, data interpretation, and conclusions are the sole responsibility of the authors. The authors further confirm that AI tools were not used to generate, fabricate, or 'hallucinate' references, and that all references have been carefully verified for accuracy.

REFERENCES

1. Atik OŞ. Corticosteroid-induced avascular necrosis of the femoral head is increased in the treatment of COVID-19 pandemic. Jt Dis Relat Surg 2023;34:757-8. doi: 10.52312/jdrs.2023.57917.
2. Gagala J, Buraczynska M, Mazurkiewicz T, Ksiazek A. Prevalence of genetic risk factors related with thrombophilia and hypofibrinolysis in patients with osteonecrosis of the femoral head in Poland. BMC Musculoskelet Disord 2013;14:264. doi: 10.1186/1471-2474-14-264.
3. Konarski W, Poboży T, Kotela A, Śliwczyński A, Kotela I, Hordowicz M, et al. Does diabetes mellitus increase the risk of avascular osteonecrosis? A systematic review and meta-analysis. Int J Environ Res Public Health 2022;19:15219. doi: 10.3390/ijerph192215219.
4. Konarski W, Poboży T, Śliwczyński A, Kotela I, Krakowiak J, Hordowicz M, et al. Avascular necrosis of femoral head-overview and current state of the art. Int J Environ Res Public Health 2022;19:7348. doi: 10.3390/ijerph19127348.
5. Petek D, Hannouche D, Suva D. Osteonecrosis of the femoral head: pathophysiology and current concepts of treatment. EFORT Open Rev 2019;4:85-97. doi: 10.1302/2058-5241.4.180036.
6. Chen Y, Miao Y, Liu K, Xue F, Zhu B, Zhang C, et al. Evolutionary course of the femoral head osteonecrosis: Histopathological - radiologic characteristics and clinical staging systems. J Orthop Translat 2021;32:28-40. doi: 10.1016/j.jot.2021.07.004.
7. Guggenbuhl P, Robin F, Cadiou S, Albert JD. Etiology of avascular osteonecrosis of the femoral head. Morphologie 2021;105:80-4. doi: 10.1016/j.morpho.2020.12.002.
8. Lespasio MJ, Sodhi N, Mont MA. Osteonecrosis of the hip: A primer. Perm J 2019;23:18-100. doi: 10.7812/TPP/18-100.
9. Powell C, Chang C, Naguwa SM, Cheema G, Gershwin ME. Steroid induced osteonecrosis: An analysis of steroid dosing risk. Autoimmun Rev 2010;9:721-43. doi: 10.1016/j.autrev.2010.06.007.
10. Wang A, Ren M, Wang J. The pathogenesis of steroid-induced osteonecrosis of the femoral head: A systematic review of the literature. Gene 2018;671:103-9. doi: 10.1016/j.gene.2018.05.091.
11. Krez A, Lane J, Heilbronner A, Park-Min KH, Kaneko K, Pannellini T, et al. Risk factors for multi-joint disease in patients with glucocorticoid-induced osteonecrosis.

Osteoporos Int 2021;32:2095-103. doi: 10.1007/s00198-021-05947-x.

12. Mont MA, Pivec R, Banerjee S, Issa K, Elmallah RK, Jones LC. High-dose corticosteroid use and risk of hip osteonecrosis: Meta-analysis and systematic literature review. J Arthroplasty 2015;30:1506-12.e5. doi: 10.1016/j.arth.2015.03.036.
13. Skoner DP. Inhaled corticosteroids: Effects on growth and bone health. Ann Allergy Asthma Immunol 2016;117:595-600. doi: 10.1016/j.anai.2016.07.043.
14. Stowe CB. The effects of pomegranate juice consumption on blood pressure and cardiovascular health. Complement Ther Clin Pract 2011;17:113-5. doi: 10.1016/j.ctcp.2010.09.004.
15. Tyagi S, Agarwal S, Agarwal S, Tyagi A Punicalagins - a large polyphenol compound found in pomegranates: a therapeutic review. Acad J Plant Sci 2012;5:45-9.
16. Chen B, Longtine MS, Riley JK, Nelson DM. Antenatal pomegranate juice rescues hypoxia-induced fetal growth restriction in pregnant mice while reducing placental cell stress and apoptosis. Placenta 2018;66:1-7. doi: 10.1016/j.placenta.2018.04.009.
17. Fouad AA, Qutub HO, Al-Melhim WN. Punicalagin alleviates hepatotoxicity in rats challenged with cyclophosphamide. Environ Toxicol Pharmacol 2016;45:158-62. doi: 10.1016/j.etap.2016.05.031.
18. Xu J, Gong H, Lu S, Deasey MJ, Cui Q. Animal models of steroid-induced osteonecrosis of the femoral head-a comprehensive research review up to 2018. Int Orthop 2018;42:1729-37. doi: 10.1007/s00264-018-3956-1.
19. Yaidikar L, Byna B, Thakur SR. Neuroprotective effect of punicalagin against cerebral ischemia reperfusion-induced oxidative brain injury in rats. J Stroke Cerebrovasc Dis 2014;23:2869-78. doi: 10.1016/j.jstrokecerebrovasdis.2014.07.020.
20. Yaidikar L, Thakur S. Punicalagin attenuated cerebral ischemia-reperfusion insult via inhibition of proinflammatory cytokines, up-regulation of Bcl-2, down-regulation of Bax, and caspase-3. Mol Cell Biochem 2015;402:141-8. doi: 10.1007/s11010-014-2321-y.
21. Dong Y, Li Y, Huang C, Gao K, Weng X. Systemic application of teriparatide for steroid induced osteonecrosis in a rat model. BMC Musculoskelet Disord 2015;16:163. doi: 10.1186/s12891-015-0589-z.
22. Lin X, Peng Q, Zhang J, Li X, Huang J, Duan S, et al. Quercetin prevents lipopolysaccharide-induced experimental preterm labor in mice and increases offspring survival rate. Reprod Sci 2020;27:1047-57. doi: 10.1007/s43032-019-00034-3.
23. Dasci MF, Yaprak Sarac E, Gok Yurttas A, Atci T, Uslu M, Acar A, et al. The effects of thymoquinone on steroid-induced femoral head osteonecrosis: An experimental study in rats. Jt Dis Relat Surg 2022;33:553-66. doi: 10.52312/jdrs.2022.752.
24. Li H, Zhang C, Zeng B. Changes in bone micro-architecture and bone mineral density following experimental osteonecrosis of femoral head by local injection of ethanol in canines. Zhongguo Xiu Fu Chong Jian Wai Ke Za Zhi 2008;22:281-9.
25. Huang L, Lu S, Bian M, Wang J, Yu J, Ge J, et al. Punicalagin attenuates TNF-α-induced oxidative damage and promotes osteogenic differentiation of bone mesenchymal stem cells by activating the Nrf2/HO-1 pathway. Exp Cell Res 2023;430:113717. doi: 10.1016/j.yexcr.2023.113717.
26. Rice JB, White AG, Scarpati LM, Wan G, Nelson WW. Long-term systemic corticosteroid exposure: A systematic literature review. Clin Ther 2017;39:2216-29. doi: 10.1016/j.clinthera.2017.09.011.
27. Huang C, Wen Z, Niu J, Lin S, Wang W. Steroid-induced osteonecrosis of the femoral head: Novel insight ınto the roles of bone endothelial cells in pathogenesis and treatment. Front Cell Dev Biol 2021;9:777697. doi: 10.3389/fcell.2021.777697.
28. Ding M, Wang Y, Sun D, Liu Z, Wang J, Li X, et al. Punicalagin pretreatment attenuates myocardial ischemia-reperfusion injury via activation of AMPK. Am J Chin Med 2017;45:53-66. doi: 10.1142/S0192415X17500057.
29. Foroutanfar A, Mehri S, Kamyar M, Tandisehpanah Z, Hosseinzadeh H. Protective effect of punicalagin, the main polyphenol compound of pomegranate, against acrylamide-induced neurotoxicity and hepatotoxicity in rats. Phytother Res 2020;34:3262-72. doi: 10.1002/ptr.6774.
30. Fouad AA, Qutub HO, Al-Melhim WN. Nephroprotection of punicalagin in rat model of endotoxemic acute kidney injury. Toxicol Mech Methods 2016;26:538-43. doi: 10.1080/15376516.2016.1211207.
31. Zhao ZQ, Bai R, Liu WL, Feng W, Zhao AQ, Wang Y, et al. Roles of oxidative DNA damage of bone marrow hematopoietic cells in steroid-induced avascular necrosis of femoral head. Genet Mol Res 2016;15. doi: 10.4238/gmr.15017706.
32. Erturk C, Diril SK, Yuzbasioglu Ozturk G, Gulcubuk A, Oran DS, Erdogan Bamac O, et al. Extra virgin olive oil alleviates articular cartilage damage and reduces ox-LDL and oxidative stress in monosodium iodoacetate-induced osteoarthritis in rats. Clin Rheumatol 2025;44:4353-65. doi: 10.1007/s10067-025-07621-7.
33. Wang Q, Ge G , Liang X, Bai J, Wang W, Zhang W, et al. Punicalagin ameliorates wear-particle-induced inflammatory bone destruction by bi-directional regulation of osteoblastic formation and osteoclastic resorption. Biomater Sci 2020;8:5157-71. doi: 10.1039/d0bm00718h.
34. Li T, Jiang G, Hu X, Yang D, Tan T, Gao Z, et al. Punicalin attenuates breast cancer-associated osteolysis by inhibiting the NF-κB signaling pathway of osteoclasts. Front Pharmacol 2021;12:789552. doi: 10.3389/fphar.2021.789552.